Development 135, 2649-2658 (2008) doi:10.1242/dev.019794

The pro-domain of the zebrafish Nodal-related protein Cyclops regulates its signaling activities

Jing Tian[1], Birgit Andrée[2], C. Michael Jones[2] and Karuna Sampath[1,3,4,*]

Nodal proteins are secreted signaling factors of the transforming growth factor β (TGFβ) family with essential roles in embryonic development in vertebrates. Mutations affecting the Nodal factors have severe consequences in mammals and fish. Furthermore, increased Nodal levels have been associated with melanoma tumor progression. Like other TGFβ-related proteins, Nodal factors consist of a pro-domain and a mature domain. The pro-domain of mouse Nodal protein stabilizes its precursor. However, the mechanisms by which the pro-domains exert their activities are unknown. Here, we characterize the zebrafish Nodal-related factor Cyclops (Cyc) and find unexpected functions for the pro-domain in regulating Cyc activity. We identified a lysosome-targeting region in the Cyc pro-domain that destabilizes the precursor and restricts Cyc activity, revealing the molecular basis for the short-range signaling activities of Cyc. We show that both the pro- and mature-domains of Cyc regulate its stability. We also characterize a mutation in the pro-domain of human NODAL (hNODAL) that underlies congenital heterotaxia. Heterologous expression of mutant hNODAL increases expression of Nodal-response genes. Our studies reveal unexpected roles for the pro-domain of the Nodal factors and provide a possible mechanism for familial heterotaxia.

KEY WORDS: Left-right asymmetry, Nodal signaling, Squint, Mature domain, Pro-domain, Zebrafish, Cyclops

INTRODUCTION

Intercellular signaling plays crucial roles not only in establishing the body plan and forming the germ layers during embryonic development, but also in cancer progression. For example, formation and patterning of the mesoderm, endoderm and ventral neural tube in vertebrates requires the function of the Nodal-related secreted signaling factors (Shen, 2007). Nodal and Nodal-related factors belong to the transforming growth factor β (TGFβ) family. Mutations affecting the Nodal factors have severe developmental consequences in mammals and fish (Shen, 2007). In addition to being a potent embryonic morphogen, Nodal has recently been shown to be a key regulator of melanoma tumorigenicity and progression (Topczewska et al., 2006). Nodal expression was found to be positively associated with melanoma tumor progression, and aggressive melanoma cell lines express more Nodal protein than lines that are not aggressive (Topczewska et al., 2006). Nodal expression has also been found in testicular cancer xenografts and in aggressive breast cancer cell lines (Adkins et al., 2003). Thus, Nodal protein levels can be an indicator of cancer progression in these cell types.

Nodal factors bind and signal through heteromeric complexes of type I and type II transmembrane serine-threonine kinase receptors (Reissmann et al., 2001; Yan et al., 2002; Yeo and Whitman, 2001). Studies in frogs, fish and mice have suggested that Nodal signaling via the type I receptor Alk4 and the type II receptors ActRIIA and ActRIIB leads to phosphorylation and nuclear accumulation of the downstream effectors Smad2 and/or Smad3 in a complex with Smad4 (Massague et al., 2005). The activated Smad complex interacts with DNA-binding proteins of the winged-helix and homeodomain families to regulate downstream target gene expression (Germain et al., 2000; Pogoda et al., 2000; Randall et al., 2004). Downstream targets of the Nodal pathway include Lefty, an inhibitor of Nodal signaling (Branford and Yost, 2002; Chen and Shen, 2004; Meno et al., 1999).

In zebrafish, the Nodal-related factors Cyclops, Squint (Sqt) and Southpaw (Spw) can induce mesoderm gene expression in ectopic overexpression assays. Analysis of mutations that affect *cyc* and *sqt* has shown that these genes have overlapping functions in the embryo during mesoderm induction (Erter et al., 1998; Feldman et al., 1998; Long et al., 2003; Rebagliati et al., 1998a; Rebagliati et al., 1998b; Sampath et al., 1998). Loss of *cyc* function results in severe deficiencies in the ventral neural tube and in cyclopia, whereas *sqt* function is required for formation of the mesendoderm and dorsal structures (Erter et al., 1998; Feldman et al., 2000; Feldman et al., 1998; Gore et al., 2005; Hagos et al., 2007; Hatta et al., 1991; Rebagliati et al., 1998b; Sampath et al., 1998; Sirotkin et al., 2000; Tian et al., 2003). Spw regulates left-right asymmetry of the visceral organs during somitogenesis (Long et al., 2003). Subsequent work also revealed differences in the signaling activities of these proteins. Whereas Cyc acts at a short-range, Sqt behaves as a long-range morphogen (Chen and Schier, 2001).

In *Xenopus*, the Nodal-related factor Xnr2 and the bone morphogenetic protein Bmp4 have short-range effects, whereas Activin functions as a long-range morphogen (Jones et al., 1996a; McDowell et al., 1997; Williams et al., 2004). The biochemical basis for the differences in activities of the various TGFβ proteins has remained unclear. Although studies on the mouse and *Xenopus* BMPs have suggested that the pro-domain may regulate mature ligand stability and processing (Constam and Robertson, 1999; Cui et al., 2001; Degnin et al., 2004; Jones et al., 1996b; Sopory et al., 2006), a recent study in zebrafish has implicated structural differences in the mature domain as being responsible (Jing et al., 2006). Furthermore, processing and glycosylation of mouse Nodal also affect the stability and signaling range of this factor (Le Good et al., 2005).

[1]Temasek Life Sciences Laboratory, 1 Research Link, National University of Singapore, Singapore 117604. [2]Institute of Medical Biology, Immunos, 8A Biomedical Grove, Singapore 138648. [3]Department of Biological Sciences, 14 Science Drive 4, National University of Singapore, Singapore 117543. [4]School of Biological Sciences, Nanyang Technological University, 30 Nanyang Drive, Singapore 637551.

*Author for correspondence (e-mail: karuna@tll.org.sg)

Accepted 6 June 2008

Here, we characterize the zebrafish Nodal-related factor Cyclops (Cyc) in detail and compare it to human NODAL (hNODAL) and zebrafish Squint (Sqt). Surprisingly, unlike the human and mouse Nodal proteins or zebrafish Sqt, processed Cyc has no discernible activity by itself, and the pro-domain of Cyc is essential for its functions. By deletion and domain-swap analysis, we identified regions in the Cyc pro-domain that regulate its expression level and stability. Interestingly, the Cyc pro-domain also plays an important role in regulating the signaling range of this factor. We identified a potential lysosome-targeting region in the Cyc pro-domain, and show that it targets the precursor for degradation. This region, when deleted, allows Cyc to function at a distance, similar to Sqt, thus revealing the molecular basis for the short-range signaling activities of Cyc. Finally, we characterize a mutation in a conserved residue in the pro-domain of hNODAL associated with congenital heterotaxia. Our results show that the pro-domain plays important roles in regulating the interactions and functions of the Nodal-related factors.

MATERIALS AND METHODS

Generation of constructs

All deletion, epitope-tagged and chimeric constructs were generated by PCR-based methods, followed by sub-cloning into the vector pCS2+, and the nucleotide sequence was confirmed (a list of primers and constructs can be provided on request). The hNODAL cDNA was amplified by RT-PCR from undifferentiated HES3 cells and cloned into the vector pCS2+. The Activin^{pro}:Cyc^{mat} chimera was generated by fusing the pro-domain of zebrafish ActivinβB with its cleavage site, to the mature domain of Cyc. The fusion constructs pCS2 *cyc^{pro}:sqt^{mat}* and pCS2 *sqt^{pro}:cyc^{mat}* were generated by PCR, with the Cyc cleavage site RRGRR in Cyc^{pro}:Sqt^{mat}, and the Sqt cleavage site RRHRR in Sqt^{pro}:Cyc^{mat}. Amino acid substitutions in the Cyc pro-domain were generated by PCR-based methods.

Zebrafish embryo injections

All experimental procedures were carried out in accordance with the guidelines of the Institutional Animal Care Use Committee at Temasek Life Sciences Laboratory. Wild-type zebrafish were maintained at 28.5°C, and embryos were obtained by standard methods for use in injection experiments. Capped mRNA was synthesized from linearized plasmids using the mMessage mMachine kit (Ambion), and 0.5 pg, 1.25 pg, 5 pg or 25 pg aliquots of capped mRNA were injected into zebrafish embryos at the one-cell stage. The embryos were fixed in 4% paraformaldehyde (PFA) at 50% epiboly and processed for in situ hybridization to detect *gsc* or *ntl* expression (Tian et al., 2003). For detecting the range of signaling, 5 or 10 pg aliquots of in vitro synthesized capped mRNA encoding Sqt, Cyc, CycΔ2, Cyc^{pro}:Sqt^{mat}, Sqt^{pro}:Cyc^{mat}, Sqt^{Cyc2}:Sqt were injected together with the lineage tracers fluorescein-dextran and biotinylated dextran (Molecular Probes) into a single cell of 64- to 128-cell zebrafish wild-type embryos. Injected embryos were fixed at 50% epiboly and analyzed by in situ hybridization to detect *gsc* and *ntl*. Biotin Dextran was detected by standard protocols (Vectastain). Stained embryos were mounted in glycerol, and images captured using a Zeiss Axioplan2 microscope equipped with a Nikon DXM 1200 color camera.

Protein expression, detection and quantification

HEK293T cells were transiently co-transfected with plasmid DNA encoding FLAG-epitope tagged Cyc or Cyc deletions, together with pEGFP as the transfection control. The cells were harvested 48 hours after transfection, and cell pellets lysed in RIPA buffer. For analysis of protein degradation, cells transfected with Myc-tagged Cyc, CycΔ2, Sqt, Sqt^{proCyc2}:Sqt, hNODAL or Bmp2b were treated with or without either the lysosomal inhibitor chloroquine (100 μM; Sigma) or the proteosome inhibitor MG132 (20 μM; Calbiochem) for 24 hours (Zhang et al., 2004). Protein concentrations were checked using a UV spectrophotometer. Each protein sample (15 μg) was separated by SDS-PAGE and transferred to a nitrocellulose membrane. Immunoblot (IB) analysis was performed using an anti-FLAG M2 mouse monoclonal antibody (Sigma) or anti-c-Myc mouse monoclonal antibody (Santa Cruz). An anti-GFP rabbit polyclonal antibody (Torrey Pines) and an anti-β-Tubulin mouse monoclonal antibody (Sigma-Aldrich) were used to detect the GFP transfection control and β-Tubulin gel loading control, respectively. Anti-mouse or anti-rabbit secondary antibodies conjugated to horseradish peroxidase (DAKO) were used, and the proteins were detected by SuperSignal West Femto Maximum Sensitivity Substrate (Pierce). The NIH Image J software package was used to quantify the proteins detected by western blots. Intensity of the individual protein bands was normalized against GFP to correct for differences in transfection efficiency between experiments and are represented as histograms.

Extraction and detection of secreted proteins

For extraction of secreted Nodal proteins, transfected HEK293T cells were incubated for 18 hours in DMEM containing 10% fetal bovine serum. pEGFP was used as the control to score transfection efficiency. Subsequently, the medium was changed to opti-MEM I reduced serum medium (GIBCO BRL), and conditioned for 36-48 hours at 37°C. The supernatants were collected and pre-cleared by centrifugation. Cell lysates were used in western blots analysis to detect control GFP expression. Secreted proteins in the cleared supernatants were concentrated with anti-Myc Monoclonal Antibody Affinity Matrix (Covance), and detected by immunoblot analysis with anti-Myc rabbit polyclonal antibodies (Santa Cruz).

Xenopus injections and scoring of left-right asymmetry

Xenopus laevis embryos were obtained by in vitro fertilization, staged and maintained according to standard protocols and institutional guidelines (Jones et al., 1996b). Embryos were injected at the four-cell stage in the dorsal right or dorsal-left blastomere with 5 μg/μl of the lineage tracer fluorescent dextran together with 25 pg of DNA encoding either wild type or mutant hNODAL or Cyc. Embryos were examined for presence and side of the fluorescent tracer at 24 hpf, sorted and cultured until stage 28 for whole-mount in situ hybridization to detect *Xpitx2* (Ryan et al., 1998). For scoring intestinal coiling, injected embryos were fixed at day 5 (Branford et al., 2000; Sampath et al., 1997). Embryos were observed using a Leica MZ 12.5 dissection microscope equipped with a Nikon DS-5M camera.

RESULTS

Cyc is inactive in the absence of its pro-domain

The mature domain of the mouse Nodal protein by itself has been shown to signal and induce downstream target gene expression in cells and embryos (Kumar et al., 2001; Le Good et al., 2005). We tested the activities of hNODAL, Sqt and Cyc by generating truncated versions (Fig. 1A) and injecting various doses into zebrafish embryos at the one-cell stage. We tested for induction of the Nodal-responsive mesendoderm gene *gsc* and the pan-mesodermal gene *ntl* at 50% epiboly. RNA encoding full-length hNODAL, Sqt, Cyc, truncated versions of Cyc, Sqt and hNODAL, and an Activin-Cyc fusion were injected. All the truncations are less active than full-length hNODAL, Cyc or Sqt. As shown previously for mouse Nodal, injection of RNA encoding only the hNODAL mature domain (hNODAL^{mat}) or Sqt (Sqt^{mat}) can induce expansion of the *gsc* and *ntl* domains at 5 pg and higher doses (Fig. 1B,C; see Tables S1 and S2 in the supplementary material). By contrast, neither the mature (Cyc^{mat}) nor the pro-domain of Cyc (Cyc^{pro}) alone induce *gsc* or *ntl* expression even at 25 pg doses. Swapping the pro-domain of Cyc with the Activin pro-domain restores partial activity at intermediate and high doses. Co-injection of Cyc^{mat} with Cyc^{pro} can induce mild expansion of the *gsc* and *ntl* expression domains, but only at very high doses (Fig. 1B,C). Therefore, unlike zebrafish Sqt and the mammalian Nodal proteins, the Cyc^{mat} domain alone is not functional by itself, and the pro-domain of Cyc is required for its activity.

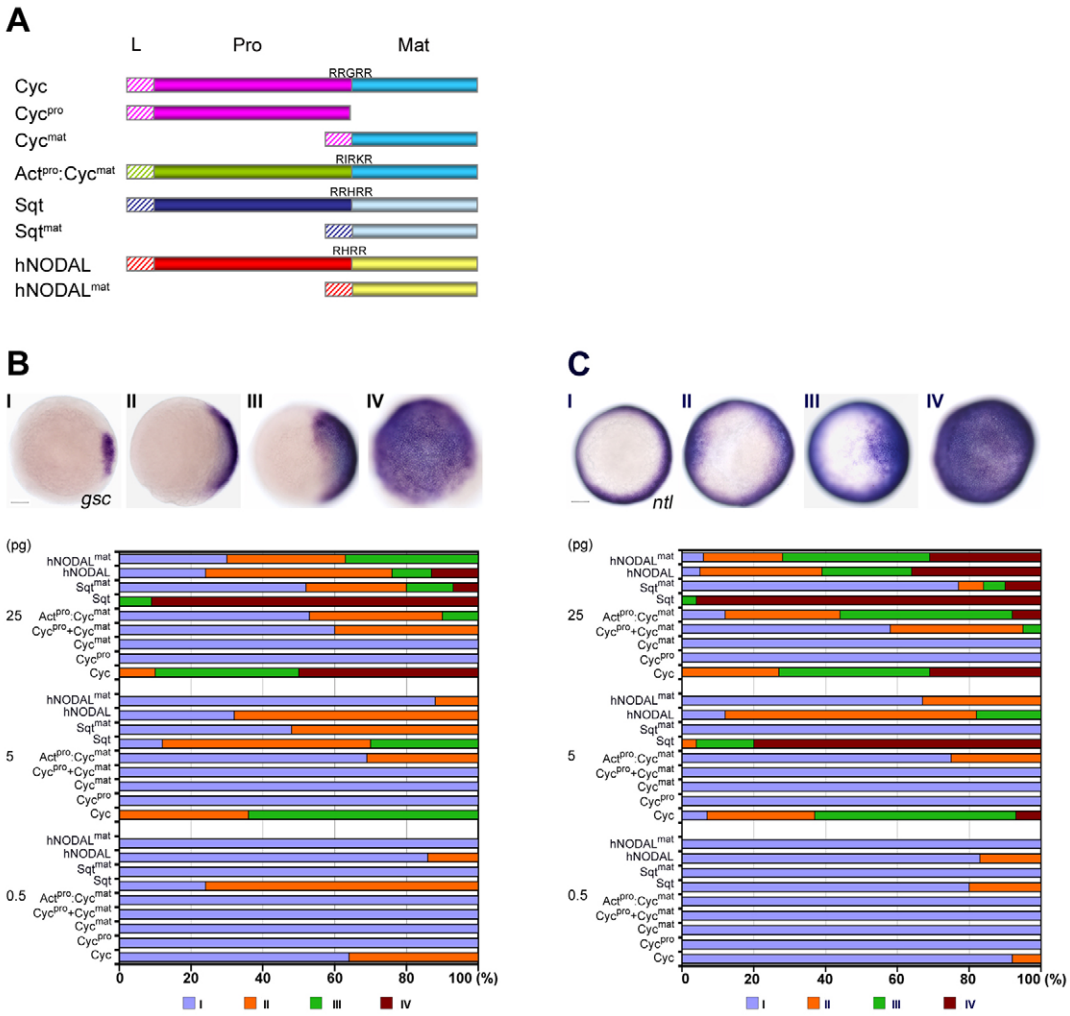

Fig. 1. The Cyc pro-domain is essential for its activity. (**A**) Schematic representation of the Cyc precursor, Cyc^{pro}, Cyc^{mat}, Activin^{pro}:Cyc^{mat} fusion, Sqt precursor, Sqt^{mat}, hNODAL precursor and hNODAL^{mat}. L indicates the leader (hatched boxes), Pro and Mat indicate the pro-domain and the mature domain, respectively. Cleavage sites between the pro- and mature regions are shown for each precursor molecule. (**B**) Analysis of induction of *gsc* by overexpression of RNA encoding Cyc, Sqt and hNODAL. RNA was injected at 0.5, 5 and 25 pg doses into one-cell wild-type embryos and expression of *gsc* was examined at 50% epiboly. Animal pole views of embryos showing endogenous *gsc* expression (I), and mild (II) or massive (III and IV) expansion of the *gsc* expression domains. Embryos were assessed and counted accordingly. Percentages for each class are shown in the histogram. Scale bar: 100 μm. (**C**) Induction of *ntl* by overexpression of RNA encoding Cyc, Sqt and hNODAL. Animal pole views of embryos showing endogenous *ntl* expression (I), mild expansion (II) or massive expansion (III and IV) of the *ntl* expression domains. Embryos were assessed and scored accordingly. Percentages for each class are shown in the histogram. Unlike hNODAL^{mat} or Sqt^{mat}, Cyc^{mat} has no discernible *gsc*- or *ntl*-inducing activity, and the Cyc pro-domain is required for its activity. Scale bar: 100 μm.

The Cyc pro-domain harbors regions that regulate its expression levels and activity

As the pro-domain of Cyc is required for activity, we generated serial deletions of 30 amino acids within this domain (Fig. 2A) in order to identify specific regions that regulate Cyc function. RNA encoding various deletion versions of Cyc was injected into one-cell zebrafish embryos and tested for induction of *gsc* (Fig. 2B; see Table S3 in the supplementary material). Deletion of regions 3, 5, 6, 10, 11 and 12 (Fig. 2A,B) from the pro-domain of Cyc causes reduced *gsc* inducing activity in comparison with full-length Cyc, and deletion of region 4 (CycΔ4) abolishes almost all activity. At higher doses, CycΔ4 can induce mild expansion of the *gsc* expression domain in some embryos (data not shown). By contrast, deletion of regions 1, 2, 7, 8 and 9 results in enhanced *gsc* inducing activity when compared with full-length Cyc. Strikingly, deletion of region 2 in the Cyc pro-domain results in a dramatic increase in activity with nearly 80% of injected embryos manifesting massive expansion of the *gsc* expression domain, 40% of which show *gsc* expression in the entire blastoderm (Fig. 2B; see Table S3 in the supplementary material).

We also examined the expression levels of FLAG epitope-tagged versions of the truncated Cyc proteins in HEK293T cells, normalized against control GFP protein levels (Fig. 2C). Significantly more protein is observed for CycΔ1 and CycΔ2 (P<0.05 as determined by the paired Student's t-test), consistent with their increased *gsc*-inducing ability in comparison with full-length Cyc. Although deletion of regions 7, 8 and 9 does not significantly alter the levels of these truncated Cyc proteins, their ability to induce

gsc is higher than full-length Cyc. Deletion of region 4 does not alter the levels of this protein even though *gsc* is not induced upon its deletion. Therefore, expression levels of the various Cyc proteins do not correlate with their ability to induce *gsc*. However, some regions (such as region 2) clearly regulate both Cyc protein level and activity.

Regulation of activity and stability by the Cyc pro-domain

Deleting the pro-domain of mouse Nodal affects its stability and range of signaling (Le Good et al., 2005). As more CycΔ2 protein is detected in comparison with Cyc, and as it is more efficient in inducing *gsc*, we examined the range of signaling of CycΔ2 (Fig. 3A,B). Embryos with cells expressing CycΔ2 show a marked increase in the range of signaling and *ntl* is induced several cell diameters from the CycΔ2 source (Fig. 3A,B). Thus, CycΔ2 behaves as a long-range morphogen, similar to Sqt. In addition, unlike Cyc, which typically does not induce *gsc* at the doses we used in the range of signaling assays, CycΔ2 induces *gsc* in 80% of injected embryos (n=41) (Fig. 3A,B). CycΔ1 also shows increased range in these assays (see Table S4 in the supplementary material), consistent with its increased expression levels (Fig. 2C), and higher activity in one-cell overexpression assays (Fig. 2B). CycΔ7, CycΔ8 and CycΔ9 levels, although not increased (Fig. 2C), show increased range of signaling, consistent with their increased activity in one-cell injection assays (see Table S4 in the supplementary material). CycΔ6, CycΔ11 and CycΔ12 also exhibit a mild increase in range of signaling assays, although overexpression of these Cyc variants at the one-cell stage does not show an increase in activity (Fig. 2B). Thus, these regions in the Cyc pro-domain have distinct effects on its activity and range of signaling.

We also swapped the pro-domains of Cyc and Sqt and tested the activity of the fusion constructs. As reported previously (Chen and Schier, 2001; Jing et al., 2006), the Sqt^{pro}:Cyc^{mat} fusion is similar to Cyc and signals at short range. However, the pro-domain of Cyc fused to Sqt^{mat} reduces the signaling range of Sqt (Fig. 3A,B). Expression of *gsc* is detected in only 27% (n=22) of embryos injected with Cyc^{pro}:Sqt^{mat}, whereas 97% of embryos that received Sqt show *gsc* expression in the receiving cells. Similarly, the signaling range, as measured by *ntl* expression, is reduced by several cell diameters when the pro-domain of Cyc is fused to Sqt^{mat} (Fig. 3A,B). Thus, the Cyc pro-domain harbors residues that restrict the activity and signaling range of the associated mature domain.

We also examined the processing of the various Cyc and Sqt proteins in HEK293T cells. Although both the processed and unprocessed forms are detected in supernatants from cells expressing Sqt, we typically do not detect unprocessed Cyc in the supernatants, and processed Cyc is detected at very low levels. Thus, unprocessed Cyc is very unstable (Fig. 3C) (Jing et al., 2006). We also examined the secreted proteins expressed from cells transfected with the cyc^{pro}:sqt^{mat} or sqt^{pro}:cyc^{mat} fusion constructs. The unprocessed and processed forms of Sqt^{pro}:Cyc^{mat} are increased relative to Cyc in supernatants of expressing cells, but the amount of processed protein detected is low in comparison to Sqt. We do not detect the Cyc^{pro}:Sqt^{mat} precursor in supernatants, and only the processed form of this protein is detected, suggesting that the Cyc^{pro} region targets the precursor for processing (Fig. 3C). Thus, the pro-domain of Cyc renders the precursor unstable and regulates its processing. In addition, Cyc^{mat} is not very stable even when fused with Sqt^{pro}. Taken together, these experiments show that Cyc is not stable in comparison with Sqt or mouse Nodal (data not shown), and that regions in the Cyc pro-domain affects its stability and signaling range.

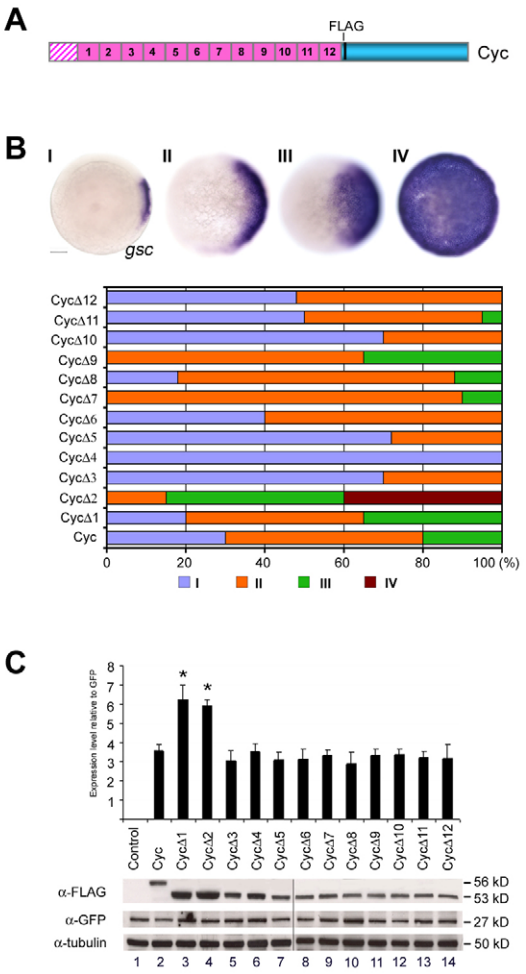

Fig. 2. Specific regions within the Cyc pro-domain regulate its expression levels and activity. (**A**) Schematic representation of the Cyc precursor. The Cyc leader sequence is shown by the hatched box, the pro-domain in pink and the mature domain in blue. Regions 1-12 are 30 amino acid stretches in the pro-domain. (**B**) Analysis of induction of *gsc* in wild-type embryos injected with 1.25 pg aliquots of RNA encoding Cyc with deletions in regions 1-12 of the pro-domain. Some deletions, such as CycΔ2 and CycΔ9, have stronger *gsc*-inducing activity than wild-type Cyc, whereas some have either no detectable activity (CycΔ4) or reduced activity. Scale bar: 100 μm. (**C**) Expression of FLAG epitope-tagged versions of the various Cyc proteins. Immunoblots on extracts of HEK293T cells expressing FLAG-tagged Cyc proteins show more CycΔ1 and CycΔ2 protein than Cyc or the other deletions. The protein samples were loaded on two gels (lanes 1-7 and 8-14, respectively), and electrophoresed in parallel. Western blots of the input proteins are shown, detected with antibodies towards the FLAG epitope for the Cyc proteins, α-GFP for transfection control and α-Tubulin for loading controls. The graph shows normalized protein expression levels relative to the GFP control, from three independent experiments (mean±s.e.m.). Asterisks indicate significant differences; P<0.05 by paired Student's t test. A representative blot is shown.

Region 2 of the Cyc pro-domain restricts Sqt activity and targets Cyc for lysosomal degradation

Region 2 of Cyc restricts its activity. As Sqt^{pro} does not harbor these residues (see Fig. S1 in the supplementary material), we tested whether swapping this region of Cyc into Sqt can affect its activity.

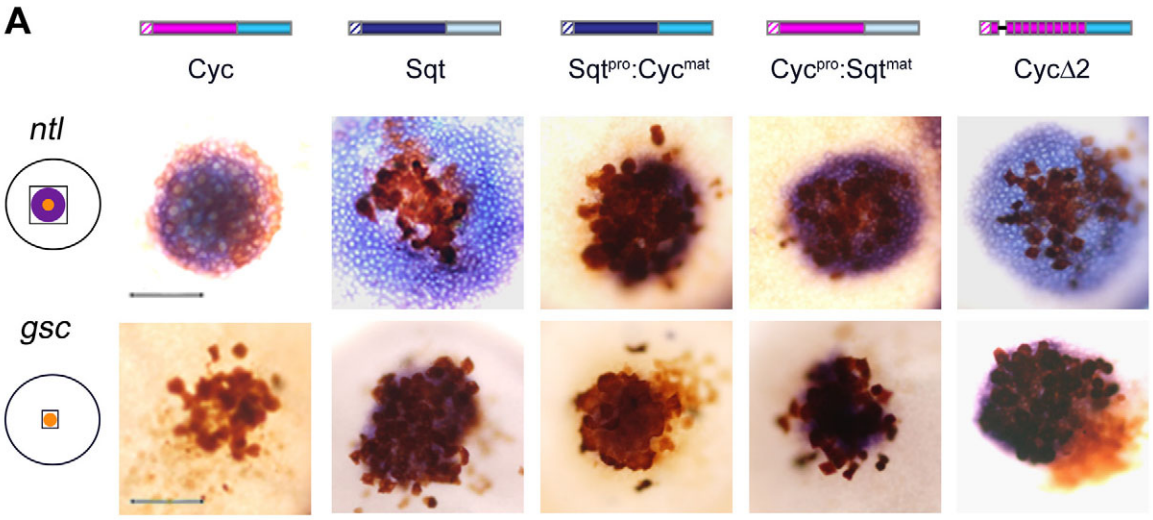

B

RNA	pg	N	*ntl* % short range in source	*ntl* % short range 1-3 cell	*ntl* % long range 4-6 cell	*ntl* % long range 6-10 cell	*ntl* % not exp.	N	*gsc* % exp.	*gsc* % not exp.
Cyc+	5	56	70	25	0	0	5	35	4	96
Sqt+	5	40	0	18	0	82	0	27	97	3
Sqt^{pro}:Cyc^{mat}	10	44	52	43	0	0	5	32	0	100
Cyc^{pro}:Sqt^{mat}	10	36	0	75	19	0	6	22	27	73
CycΔ2	5	45	25	14	55	0	6	41	80	20

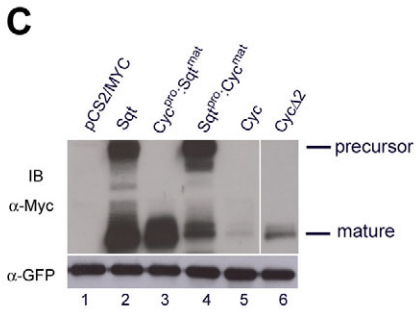

Fig. 3. The Cyc pro-domain regulates processing, stability and signaling. (**A**) Schematic representation of Cyc, Sqt, Sqt^{pro}:Cyc^{mat}, Cyc^{pro}:Sqt^{mat} and CycΔ2. Hatched boxes indicate the leader sequences, the Cyc pro-domain is shown in pink, the Sqt pro-domain in dark blue, the Sqt mature domain in pale blue and the Cyc mature domain in mid-blue. RNA encoding the various Nodal-related proteins (5-10 pg) was injected into one-cell at the 64- to 128-cell stage together with a lineage tracer (brown). Range of signaling was examined by in situ hybridization to detect *ntl* (blue, top panel) and *gsc* (blue-brown, bottom panel) expression. All in situ panels show the boxed area indicated in the schematic of the embryo shown in the left. Expression of *ntl* is seen in all clones, whereas *gsc* expression is detected in the clones expressing Sqt, Cyc^{pro}:Sqt^{mat} and CycΔ2, but not Cyc or Sqt^{pro}:Cyc^{mat}. In comparison with Cyc, the range of activity of CycΔ2 is markedly expanded, as observed by expression of *ntl*, and CycΔ2 behaves similar to Sqt in inducing *gsc*. The Sqt^{pro}:Cyc^{mat} fusion behaves like Cyc in the expression of both *ntl* and *gsc*, whereas *ntl* expression shows that Cyc^{pro}:Sqt^{mat} has reduced signaling activity compared with Sqt. Expression of *gsc* is detected in some Cyc^{pro}:Sqt^{mat}-injected embryos. All embryos were viewed from the animal pole. Scale bar: 100 μm. (**B**) Table summarizing *ntl* and *gsc* expression in the range of signaling assays. For *gsc*, the embryos were classified as with or without ectopic expression. The induction of *ntl* was classified as short range (expression in injected cells to three-cell diameters from injected source), long range (expression in cells that are 4-10 cell diameters from source) or not expressing. The amount of injected mRNA (pg), the total number of embryos examined (N) and the percentage of embryos in each category are indicated. (**C**) Supernatants from HEK293T cells expressing Myc-tagged Sqt, Cyc^{pro}:Sqt^{mat}, Sqt^{pro}:Cyc^{mat}, Cyc and CycΔ2 proteins. Both unprocessed (~46 kDa) and processed (~17 kDa) forms of Sqt are detected. The Cyc precursor is not detected, whereas substantial amounts of the Sqt^{pro}:Cyc^{mat} precursor (~45 kDa) are detected. For Cyc^{pro}:Sqt^{mat}, no precursor is detected. Very low levels of processed Cyc^{mat} (~16 kDa) is detected from supernatants of cell expressing Cyc, and marginally higher amounts of processed Cyc is detected in the CycΔ2 lane (~16 kDa). The samples were electrophoresed on a SDS-PAGE gel; lane 6 (CycΔ2) is from a different part of the same gel. Expression of the transfection control GFP in cell lysates is shown in the lower panel.

Injection of one-cell embryos with chimeric Sqt ($Sqt^{proCyc2}$:Sqt) containing the Cyc region 2 residues results in reduced *gsc* and *ntl* inducing ability in comparison with Sqt (Fig. 4A-C). In contrast to embryos injected with sqt RNA that show substantial expansion of the *gsc* and *ntl* expression domains (Fig. 4B,C; see Tables S5 and S6 in the supplementary material), embryos injected with $sqt^{proCyc2}$:sqt RNA manifest only modest expansion of the *gsc* and *ntl* expression domains (see Tables S5 and S6 in the supplementary material). We also examined the range of signaling of $Sqt^{proCyc2}$:Sqt in comparison with Cyc and Sqt. Although *ntl* expression is induced by cells expressing $Sqt^{proCyc2}$:Sqt, the range of *ntl* expression is reduced in comparison with embryos expressing Sqt (Fig. 4D; see Table S7 in the supplementary material). Furthermore, *gsc* expression is not detected in most embryos expressing $Sqt^{proCyc2}$:Sqt (88%; n=41), similar to embryos injected with RNA encoding Cyc (Fig. 4D; see Table S7 in the supplementary material). Supernatants from HEK293T cells expressing $Sqt^{proCyc2}$:Sqt also show that both unprocessed and processed Sqt protein levels are reduced (Fig. 4E) in comparison with cells expressing Sqt.

Region 2 in Cyc harbors a YRHY motif, which bears some similarity to the consensus endosomal/lysosomal targeting sequence YXXΦ (Bonifacino and Dell'Angelica, 1999) (see Fig. S1 in the supplementary material). Therefore, we tested if treatment with the lysosomal inhibitor, chloroquine, can stabilize the precursors. Although Cyc is stabilized by chloroquine treatment for 24 hours, CycΔ2 does not show a significant difference in the

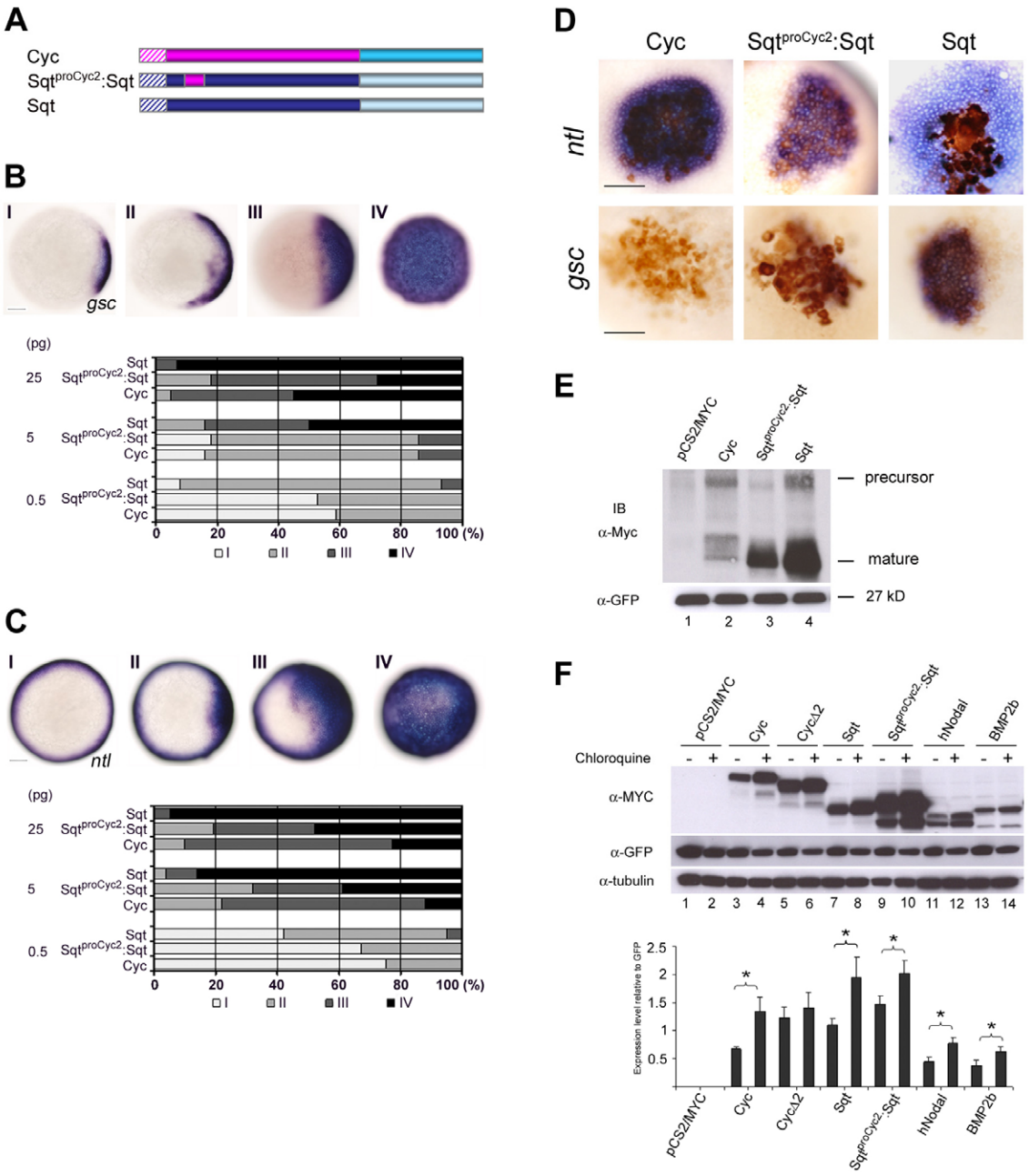

Fig. 4. Region 2 of the Cyc pro-domain renders chimeric Sqt unstable, and targets the precursor for degradation. (**A**) Schematic representation of Cyc, Sqt and Sqt^{proCyc2}:Sqt. Hatched boxes indicate the leader sequences, the Cyc pro-domain is shown in pink, the Sqt pro-domain in dark blue, the Sqt mature domain in pale blue and the Cyc mature domain in mid-blue. (**B**,**C**) Analysis of induction of *gsc* (B) or *ntl* (C) in wild-type embryos injected at the one-cell stage with 0.5, 5 or 25 pg of RNA encoding Cyc, Sqt or Sqt^{proCyc2}:Sqt. Animal pole views of embryos at 50% epiboly showing endogenous *gsc* or *ntl* expression (I), and mild (II) or massive (III and IV) expansion of the *gsc* or *ntl* expression domains. Embryos were assessed and counted, and percentages for each class are shown in histograms. Scale bars: 100 μm. (**D**) 5 pg of RNA encoding Cyc, Sqt or Sqt^{proCyc2}:Sqt was injected into one cell at the 64- to 128-cell stage together with a lineage tracer (brown). Range of signaling was examined by in situ hybridization to detect *ntl* (blue, top panel) and *gsc* (blue-brown, bottom panel) expression. The Sqt^{proCyc2}:Sqt fusion behaves like Cyc, with its reduced *ntl* expression domain and the lack of *gsc* expression in most embryos (see Table S7 in the supplementary material). Scale bars: 100 μm. (**E**) Supernatants from HEK293T cells expressing Myc-tagged Sqt, Cyc and Sqt^{proCyc2}:Sqt proteins. Both unprocessed (~46 kDa) and processed (~17 kDa) forms of Sqt are detected. For Sqt^{proCyc2}:Sqt, the precursor is typically not detected and the processed Sqt (~17 kDa) protein levels are reduced. The processed form of Cyc (~16 kDa) is detected at very low levels. Supernatants from cells expressing pCS2Myc were used as negative control. GFP expression in the cell lysates was used to measure transfection efficiency. (**F**) Immunoblots to detect Myc-tagged Cyc (~58 kDa), CycΔ2 (~55 kDa), Sqt (~46 kDa), Sqt^{proCyc2}:Sqt (~46 kDa), hNODAL (~41 kDa) or Bmp2b (~48 kDa) in extracts of cells grown in the presence or absence of the lysosomal inhibitor chloroquine. CycΔ2 expression is not significantly altered by chloroquine treatment. By comparison, Cyc and the other proteins are stabilized by chloroquine. GFP was used as the transfection control and tubulin was used as the loading control. The histogram shows normalized protein expression levels relative to the GFP control, from three independent experiments (mean±s.e.m.). The asterisks (*) indicate significant differences (P<0.05 as determined by paired Student's t-test) between cells not treated versus those treated with the lysosomal inhibitor for 24 hours. A representative gel from three independent experiments is shown.

presence of chloroquine (Fig. 4F). By contrast, CycΔ2 is stabilized by treatments for 24 hours with the proteosome inhibitor MG132, similar to the other proteins (see Fig. S2 in the supplementary material). We detected more Sqt, Sqt^{proCyc2}:Sqt, hNODAL and Bmp2b protein in the presence of chroloquine, indicating that these TGFβ-related proteins may also be targeted to the lysosome. Thus, region 2 of the Cyc pro-domain can render the precursors less stable, and restricts their signaling activity by targeting to the lysosome for degradation.

A mutation in the pro-domain of hNODAL renders it more active and is responsible for familial heterotaxia

A mutation in the human *NODAL* gene has been reported in members of a family with left-right asymmetry defects (Casey, 1998; Gebbia et al., 1997). This mutation affects an arginine residue in the pro-domain of hNODAL (see Fig. S1 in the supplementary material). We tested the activity of mutant hNODAL^{R183Q} in comparison with that of wild-type hNODAL. Injection of the mutant

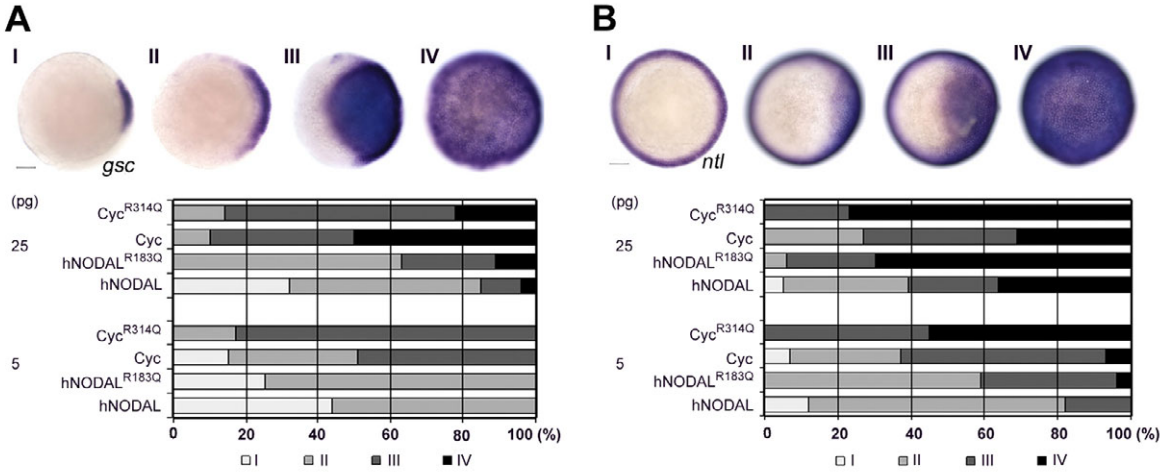

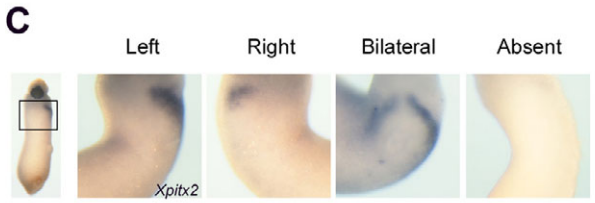

DNA	Dose (pg)	Injected Side	N	% left *Xpitx2*	% right *Xpitx2*	% bilateral *Xpitx2*	% no *Xpitx2* exp.
hNODAL	25	left	44	82	0	5	13
	25	right	36	31	22	22	25
hNODAL^{R183Q}	25	left	53	74	2	11	13
	25	right	44	25	39	16	20
Cyc	25	left	48	77	0	2	21
	25	right	46	50	7	17	26
Cyc^{R314Q}	25	left	49	55	0	6	39
	25	right	43	21	19	30	30

D

DNA & Dose (pg)	Injected side	N	% normal	% reversal	% abnormal	% heterotaxic
hNODAL 25pg	left	50	82	4	8	6
	right	45	44	16	22	18
hNODAL^{R183Q} 25pg	left	59	81	3	9	7
	right	41	41	32	20	7

Fig. 5. Mutation of a conserved arginine residue in hNODAL renders the protein more active and can induce left-right asymmetry defects. (**A**,**B**) Cyc^{R314Q} and hNODAL^{R183Q} are more active than Cyc and hNODAL. Zebrafish embryos at the one-cell stage were injected with 5 or 25 pg of RNA encoding either Cyc, Cyc^{R314Q}, hNODAL or hNODAL^{R183Q}. Expression of *gsc* (A) or *ntl* (B) was examined at 50% epiboly. The Arg-Gln mutations render Cyc^{R314Q} and hNODAL^{R183Q} more active than the wild-type proteins. Animal pole views shown. Scale bar: 100 μm. (**C**) Overexpression of Cyc^{R314Q} and hNODAL^{R183Q} in *Xenopus* embryos causes perturbations in left-sided expression of *Xpitx2*. *Xenopus* embryos at the four-cell stage were injected with 25 pg of DNA expression constructs encoding either Cyc, Cyc^{R314Q}, hNODAL or hNODAL^{R183Q} in the dorsal-left or dorsal-right blastomeres and cultured until stage 28 and processed for in situ hybridization to detect *Xpitx2* expression. Embryos were scored as left, right, bilateral or no *Xpitx2* expression. Ventral views of stage 28 embryos with *Xpitx2* expression in the cardiac primordia are shown. Injections of hNODAL^{R183Q} or Cyc^{R314Q} can induce right-sided, bilateral or no *Xpitx2* expression at a higher frequency than observed after injections of hNODAL or Cyc. (**D**) Gut looping is also perturbed by injection of hNODAL^{R183Q}. *Xenopus* embryos at the four-cell stage were injected with 25 pg of DNA encoding either hNODAL or hNODAL^{R183Q} in the dorsal-left or dorsal-right blastomeres and cultured until stage 45 and scored for the direction of intestinal coiling. Injected embryos manifested either normal, reversed or abnormal looping. In some embryos, heterotaxia of intestinal coiling and cardiac laterality was observed. Right-sided injections of hNODAL^{R183Q} increase the frequency of reversed intestinal coiling in comparison with hNODAL.

hNODAL^{R183Q} RNA into zebrafish embryos at the one-cell stage causes increased expansion of the *gsc* and *ntl* expression domains, in comparison with wild-type hNODAL RNA at the same doses (Fig. 5A,B). The pro-domain of the zebrafish Nodal factor Cyc also harbors this Arg residue. We also tested mutant Cyc harboring a mutation in the conserved residue (see Fig. S1 in the supplementary material). Upon injection of low doses of Cyc^{R314Q} RNA into zebrafish embryos, we observed a similar increase in activity compared with Cyc (Fig. 5A,B). Thus, this Arg residue may have conserved functions in the zebrafish Nodal and hNODAL proteins.

We then tested the ability of the mutant hNODAL^{R183Q} and Cyc^{R314Q} proteins to perturb left-right asymmetry in *Xenopus* embryos and compared it with that of wild-type hNODAL or Cyc DNA. Left- as well as right-sided microinjections of mutant hNODAL^{R183Q} or Cyc^{R314Q} DNA expression constructs into *Xenopus* embryos can induce perturbations in expression of the Nodal target gene, X*pitx2* (Fig. 5C). By contrast, left-sided injection of the wild-type hNODAL or Cyc DNA does not cause right-sided X*pitx2* expression at the same doses. In addition, right-sided expression of mutant hNODAL^{R183Q} or Cyc^{R314Q} results in a higher proportion of either bilateral or right-sided X*pitx*2 expression in comparison with hNODAL or Cyc. We also examined the direction of intestinal coiling in *Xenopus* embryos injected with DNA expression constructs encoding either hNODAL or hNODAL^{R183Q}. The proportion of embryos manifesting normal or reversed intestinal coiling is comparable in embryos injected on the left side with either wild type hNODAL or mutant hNODAL^{R183Q}. However, right-sided expression of hNODAL^{R183Q} leads to a higher frequency of reversal in intestinal coiling in comparison with hNODAL (Fig. 5D). Thus, the proportion of embryos manifesting perturbations in X*pitx2* expression and reversal of gut looping is increased in embryos injected with mutant hNODAL^{R183Q} DNA. Taken together, the results from overexpression in zebrafish and *Xenopus* embryos suggest that the mutation in the hNODAL pro-domain can lead to gain-of-function activity and left-right asymmetry defects.

DISCUSSION

Although the Nodal-related proteins are similar in that they can act as mesoderm inducers, there appear to be some differences in the activities of these factors in embryos. The *Xenopus* Xnr-1 and Xnr-2 proteins differ in their ability to induce mesoderm and to affect left-right asymmetry (Jones et al., 1995; Sampath et al., 1997). Genetic analysis in zebrafish has shown that Cyc has cell autonomous as well as non-autonomous functions, and the cell autonomous activity of Cyc is particularly important in development of the ventral neural tube (Hatta et al., 1991; Sampath et al., 1998). Other experiments have suggested that Cyc acts over a short range, whereas Sqt behaves as a long-range morphogen. The mouse Nodal protein is known to have long-range signaling activities (Chen and Schier, 2001; Le Good et al., 2005). The biochemical basis for these differences is just beginning to be elucidated and a recent study showed that acidic residues in the mature domain of Cyc contribute towards its short-range activity (Jing et al., 2006). Although Cyc and Sqt share 68% identity and 78% sequence similarity in their mature domains, their pro-domains are more divergent (Erter et al., 1998; Rebagliati et al., 1998a). In particular, the Cyc pro-domain has several proline-rich regions that are not shared by any of the other vertebrate Nodal-related factors (Hudson and Yasuo, 2005; Jones et al., 1995; Morokuma et al., 2002; Rebagliati et al., 1998a; Sampath et al., 1998; Tian et al., 2003; Toyama et al., 1995; Yu et al., 2002; Zhou et al., 1993). Although it is not clear how this region evolved, the presence of the proline-rich repeats is suggestive of insertion by retroposon-like elements. Our experiments where we disrupt the Cyc pro-domain via deletions and point mutations indicate that this region of Cyc contributes to the instability of this Nodal-related factor. Similar findings have been reported for mouse Nodal. Although expression of wild-type Bmp4 could be detected in COS cells, no mature BMP4 was detected when expressed as a chimeric Nodal^{pro}:BMP4^{mat} protein, and, conversely, fusion of Dorsalin^{pro} to Nodal ^{mat} had a stabilizing effect on Nodal^{mat} expression (Constam and Robertson, 1999). Interestingly, in our biochemical studies, we typically do not detect the Cyc precursor, suggesting that the Cyc precursor is rapidly turned over. Similar findings have been reported for a Cyc-GFP fusion protein expressed in COS cells (Jing et al., 2006). Thus, regions in the Cyc pro- as well as Cyc mature-domain are responsible for the overall instability of this Nodal-related factor, and this is probably the reason that Cyc has only short-range signaling activities in embryos.

Remarkably, swapping the pro-domain of Sqt with that of Cyc restricts the long-range signaling ability of Sqt^{mat}. A cleavage-resistant form of mouse Nodal can induce expression of Bmp4 in cells at a distance from its source (Ben-Haim et al., 2006). This raises the possibility that the zebrafish Nodal precursors may act at a distance from their source, and the Cyc pro-domain reduces the signaling range of the Cyc:Sqt precursor. In addition, we observed that no secreted precursor of the Cyc^{pro}:Sqt^{mat} fusion is detected, further verifying that the pro-domain of Cyc contributes to the turnover of the precursor proteins. This contrasts with previous reports using a Cyc^{pro}:Sqt^{mat}GFP fusion that found that activity of a Cyc:Sqt chimera is indistinguishable from that of Sqt (Jing et al., 2006). We cannot explain the reason for the difference in activity of the Cyc:Sqt fusion observed by the two groups, but one possibility is that the larger GFP epitope tag used by Jing et al. may allow their fusion protein to be more stable than our Cyc:Sqt fusion. As observed by Jing et al., we also find that the Sqt^{pro}:Cyc^{mat} fusion protein is, by and large, similar in activity to Cyc. In some injected embryos (43%; n=44), we observed a mild expansion (two or three cells) of the *ntl* expression domain. Interestingly, we detect substantial amounts of the Sqt^{pro}:Cyc^{mat} precursor in supernatants of expressing cells, whereas secreted Cyc precursor is typically not detected in our assays. However, the amount of processed Cyc^{mat} from the Sqt:Cyc fusion is low, similar to Cyc. Therefore, although the Sqt pro-domain can stabilize the Sqt^{pro}:Cyc^{mat} precursor, mature Cyc is inherently unstable. These findings also point towards fundamental differences between the pro-domains of Cyc and Sqt.

Surprisingly, unlike zebrafish Sqt or the mammalian Nodal factors, the Cyc mature domain by itself has no activity. Swapping the Cyc pro-domain with that of Activin restored some activity, but not to the levels observed with Cyc, indicating that the Activin:Cyc chimera is less active than wild-type Cyc. Thus, the Cyc pro-domain is vital for its functions. We typically detect less processed Cyc in comparison to processed Sqt and mouse Nodal in culture supernatants. Therefore, the lack of activity of Cyc^{mat} may be because it is much more unstable than processed Sqt and mouse Nodal. We also find it difficult to detect hNODAL protein in our assays (data not shown) (Topczewska et al., 2006), indicating similarities between Cyc and hNODAL proteins. As increased hNODAL levels have been associated with tumor progression, the turnover of hNODAL may be an important step in regulation of its activities.

We identified a region in the N terminus of the Cyc pro-domain (region 2), which when deleted increases Cyc activity and allows it to function as a long-range mesoderm inducer, similar to Sqt and

mouse Nodal. How does region 2 regulate Cyc protein activity? One possibility is that the residues in region 2 target the precursor for degradation, leading to its rapid turnover in embryos. In support of this possibility, region 2 in Cyc harbors a YRHY motif, which has some similarity to consensus endosome/lysosome-targeting sequences (Bonifacino and Dell'Angelica, 1999). Removal of this region makes Cyc more stable and, conversely, a chimeric Sqt protein that contains region 2 of the Cyc pro-domain is less stable and less active than Sqt, and sensitive to the lysosomal inhibitor chloroquine. Studies with *Xenopus* Bmp4 have also shown that the processing of BMP4 is regulated by the pro-domain of this factor, and cleavage within the pro-domain directs degradation of mature Bmp4 (Sopory et al., 2006). Therefore, it is conceivable that these residues in the Cyc pro-domain regulate its degradation. Nonetheless, we cannot rule out other mechanisms that may regulate Cyc protein synthesis, secretion or processing. For example, glycosylation regulates the stability of mouse Nodal protein (Le Good et al., 2005). There are four predicted N-glycosylation sites in Cyc, all of which reside in the Cyc pro-domain, in regions 1, 2, 4 and 11, respectively. Of the Cyc deletions in regions with the predicted glycosylation sites, CycΔ1 and CycΔ2 exhibit enhanced activity of Cyc, whereas CycΔ11 and CycΔ4 display reduced and no activity, respectively. Therefore, we do not observe a direct correlation between glycosylation sites and Cyc stability or activity. However, as our experiments make use of deletions, it remains possible that glycosylation may regulate Cyc activity.

A conserved Arg residue in the hNODAL and Cyc pro-domains, when mutated, causes increased activity of these Nodal proteins. It is not clear whether the R>Q mutation increases hNODAL activity by stabilizing the protein or by regulating its interactions with other components of the NODAL signaling pathway. We find that this increase in activity is modest, so it may allow germ layer formation and patterning in early embryos. Nonetheless, this modest increase in activity is sufficient to cause laterality defects. Human laterality defects have been found to be associated with loss-of-function mutations in the Nodal co-receptor CFC1 (Cryptic), the zinc-finger transcription factor Zic3, the Nodal antagonist Leftyb and the type II activin receptor Actr2b (Bamford et al., 2000; Gebbia et al., 1997; Kosaki, K. et al., 1999; Kosaki, R. et al., 1999). As expression of the mutant hNODAL protein can enhance laterality defects in frogs, it is likely that it is the gain-of-function activity of the mutant hNODAL that is responsible for the heterotaxia defects found in individuals harboring this mutation. Thus, the pro-domain of the Nodal factors not only regulates their stability, but is also important for other aspects of signaling by these factors. Understanding the precise mechanisms by which the pro-domain influences Nodal activity will provide further insights into the regulation of these essential signaling factors.

We thank Ray Dunn, Aniket Gore, Sudipto Roy and members of the Sampath laboratory for discussions and suggestions; Ray Dunn for human ES cell RNA; Chan Aye Thu, Wang Xin, Siew Peng Tan, Hong Xin and Helen Ngoc Bao Quach for technical assistance; Shi Min Lim for assistance with the manuscript and figures; Srinivas Ramasamy and the TLL Bioinformatics core; and the TLL sequencing and fish facilities for support. B.A. and C.M.J. are supported by A*STAR, Singapore. Work in the laboratory of K.S. is supported by Temasek Life Sciences Laboratory, Singapore.

Supplementary material

Supplementary material for this article is available at
http://dev.biologists.org/cgi/content/full/135/15/2649/DC1

References

Adkins, H. B., Bianco, C., Schiffer, S. G., Rayhorn, P., Zafari, M., Cheung, A. E., Orozco, O., Olson, D., De Luca, A., Chen, L. L. et al. (2003). Antibody blockade of the Cripto CFC domain suppresses tumor cell growth in vivo. *J. Clin. Invest.* **112**, 575-587.

Bamford, R. N., Roessler, E., Burdine, R. D., Saplakoglu, U., dela Cruz, J., Splitt, M., Goodship, J. A., Towbin, J., Bowers, P., Ferrero, G. B. et al. (2000). Loss-of-function mutations in the EGF-CFC gene CFC1 are associated with human left-right laterality defects. *Nat. Genet.* **26**, 365-369.

Ben-Haim, N., Lu, C., Guzman-Ayala, M., Pescatore, L., Mesnard, D., Bischofberger, M., Naef, F., Robertson, E. J. and Constam, D. B. (2006). The nodal precursor acting via activin receptors induces mesoderm by maintaining a source of its convertases and BMP4. *Dev. Cell* **11**, 313-323.

Bonifacino, J. S. and Dell'Angelica, E. C. (1999). Molecular bases for the recognition of tyrosine-based sorting signals. *J. Cell Biol.* **145**, 923-926.

Branford, W. W. and Yost, H. J. (2002). Lefty-dependent inhibition of Nodal- and Wnt-responsive organizer gene expression is essential for normal gastrulation. *Curr. Biol.* **12**, 2136-2141.

Branford, W. W., Essner, J. J. and Yost, H. J. (2000). Regulation of gut and heart left-right asymmetry by context-dependent interactions between xenopus lefty and BMP4 signaling. *Dev. Biol.* **223**, 291-306.

Casey, B. (1998). Two rights make a wrong: human left-right malformations. *Hum. Mol. Genet.* **7**, 1565-1571.

Chen, C. and Shen, M. M. (2004). Two modes by which Lefty proteins inhibit nodal signaling. *Curr. Biol.* **14**, 618-624.

Chen, Y. and Schier, A. F. (2001). The zebrafish Nodal signal Squint functions as a morphogen. *Nature* **411**, 607-610.

Constam, D. B. and Robertson, E. J. (1999). Regulation of bone morphogenetic protein activity by pro domains and proprotein convertases. *J. Cell Biol.* **144**, 139-149.

Cui, Y., Hackenmiller, R., Berg, L., Jean, F., Nakayama, T., Thomas, G. and Christian, J. L. (2001). The activity and signaling range of mature BMP-4 is regulated by sequential cleavage at two sites within the prodomain of the precursor. *Genes Dev.* **15**, 2797-2802.

Degnin, C., Jean, F., Thomas, G. and Christian, J. L. (2004). Cleavages within the prodomain direct intracellular trafficking and degradation of mature bone morphogenetic protein-4. *Mol. Biol. Cell* **15**, 5012-5020.

Erter, C. E., Solnica-Krezel, L. and Wright, C. V. (1998). Zebrafish nodal-related 2 encodes an early mesendodermal inducer signaling from the extraembryonic yolk syncytial layer. *Dev. Biol.* **204**, 361-372.

Feldman, B., Gates, M. A., Egan, E. S., Dougan, S. T., Rennebeck, G., Sirotkin, H. I., Schier, A. F. and Talbot, W. S. (1998). Zebrafish organizer development and germ-layer formation require nodal-related signals. *Nature* **395**, 181-185.

Feldman, B., Dougan, S. T., Schier, A. F. and Talbot, W. S. (2000). Nodal-related signals establish mesendodermal fate and trunk neural identity in zebrafish. *Curr. Biol.* **10**, 531-534.

Gebbia, M., Ferrero, G. B., Pilia, G., Bassi, M. T., Aylsworth, A., Penman-Splitt, M., Bird, L. M., Bamforth, J. S., Burn, J., Schlessinger, D. et al. (1997). X-linked situs abnormalities result from mutations in ZIC3. *Nat. Genet.* **17**, 305-308.

Germain, S., Howell, M., Esslemont, G. M. and Hill, C. S. (2000). Homeodomain and winged-helix transcription factors recruit activated Smads to distinct promoter elements via a common Smad interaction motif. *Genes Dev.* **14**, 435-451.

Gore, A. V., Maegawa, S., Cheong, A., Gilligan, P. C., Weinberg, E. S. and Sampath, K. (2005). The zebrafish dorsal axis is apparent at the four-cell stage. *Nature* **438**, 1030-1035.

Hagos, E. G., Fan, X. and Dougan, S. T. (2007). The role of maternal Activin-like signals in zebrafish embryos. *Dev. Biol.* **309**, 245-258.

Hatta, K., Kimmel, C. B., Ho, R. K. and Walker, C. (1991). The cyclops mutation blocks specification of the floor plate of the zebrafish central nervous system. *Nature* **350**, 339-341.

Hudson, C. and Yasuo, H. (2005). Patterning across the ascidian neural plate by lateral Nodal signalling sources. *Development* **132**, 1199-1210.

Jing, X. H., Zhou, S. M., Wang, W. Q. and Chen, Y. (2006). Mechanisms underlying long- and short-range nodal signaling in Zebrafish. *Mech. Dev.* **123**, 388-394.

Jones, C. M., Kuehn, M. R., Hogan, B. L., Smith, J. C. and Wright, C. V. (1995). Nodal-related signals induce axial mesoderm and dorsalize mesoderm during gastrulation. *Development* **121**, 3651-3662.

Jones, C. M., Armes, N. and Smith, J. C. (1996a). Signalling by TGF-beta family members: short-range effects of Xnr-2 and BMP-4 contrast with the long-range effects of activin. *Curr. Biol.* **6**, 1468-1475.

Jones, C. M., Dale, L., Hogan, B. L., Wright, C. V. and Smith, J. C. (1996b). Bone morphogenetic protein-4 (BMP-4) acts during gastrula stages to cause ventralization of Xenopus embryos. *Development* **122**, 1545-1554.

Kosaki, K., Bassi, M. T., Kosaki, R., Lewin, M., Belmont, J., Schauer, G. and Casey, B. (1999). Characterization and mutation analysis of human LEFTY A and LEFTY B, homologues of murine genes implicated in left-right axis development. *Am. J. Hum. Genet.* **64**, 712-721.

Kosaki, R., Gebbia, M., Kosaki, K., Lewin, M., Bowers, P., Towbin, J. A. and Casey, B. (1999). Left-right axis malformations associated with mutations in

ACVR2B, the gene for human activin receptor type IIB. *Am. J. Med. Genet.* **82**, 70-76.
Kumar, A., Novoselov, V., Celeste, A. J., Wolfman, N. M., ten Dijke, P. and Kuehn, M. R. (2001). Nodal signaling uses activin and transforming growth factor-beta receptor-regulated Smads. *J. Biol. Chem.* **276**, 656-661.
Le Good, J. A., Joubin, K., Giraldez, A. J., Ben-Haim, N., Beck, S., Chen, Y., Schier, A. F. and Constam, D. B. (2005). Nodal stability determines signaling range. *Curr. Biol.* **15**, 31-36.
Long, S., Ahmad, N. and Rebagliati, M. (2003). The zebrafish nodal-related gene southpaw is required for visceral and diencephalic left-right asymmetry. *Development* **130**, 2303-2316.
Massague, J., Seoane, J. and Wotton, D. (2005). Smad transcription factors. *Genes Dev.* **19**, 2783-2810.
McDowell, N., Zorn, A. M., Crease, D. J. and Gurdon, J. B. (1997). Activin has direct long-range signalling activity and can form a concentration gradient by diffusion. *Curr. Biol.* **7**, 671-681.
Meno, C., Gritsman, K., Ohishi, S., Ohfuji, Y., Heckscher, E., Mochida, K., Shimono, A., Kondoh, H., Talbot, W. S., Robertson, E. J. et al. (1999). Mouse Lefty2 and zebrafish antivin are feedback inhibitors of nodal signaling during vertebrate gastrulation. *Mol. Cell* **4**, 287-298.
Morokuma, J., Ueno, M., Kawanishi, H., Saiga, H. and Nishida, H. (2002). HrNodal, the ascidian nodal-related gene, is expressed in the left side of the epidermis, and lies upstream of HrPitx. *Dev. Genes Evol.* **212**, 439-446.
Pogoda, H. M., Solnica-Krezel, L., Driever, W. and Meyer, D. (2000). The zebrafish forkhead transcription factor FoxH1/Fast1 is a modulator of nodal signaling required for organizer formation. *Curr. Biol.* **10**, 1041-1049.
Randall, R. A., Howell, M., Page, C. S., Daly, A., Bates, P. A. and Hill, C. S. (2004). Recognition of phosphorylated-Smad2-containing complexes by a novel Smad interaction motif. *Mol. Cell. Biol.* **24**, 1106-1121.
Rebagliati, M. R., Toyama, R., Fricke, C., Haffter, P. and Dawid, I. B. (1998a). Zebrafish nodal-related genes are implicated in axial patterning and establishing left-right asymmetry. *Dev. Biol.* **199**, 261-272.
Rebagliati, M. R., Toyama, R., Haffter, P. and Dawid, I. B. (1998b). cyclops encodes a nodal-related factor involved in midline signaling. *Proc. Natl. Acad. Sci. USA* **95**, 9932-9937.
Reissmann, E., Jornvall, H., Blokzijl, A., Andersson, O., Chang, C., Minchiotti, G., Persico, M. G., Ibanez, C. F. and Brivanlou, A. H. (2001). The orphan receptor ALK7 and the Activin receptor ALK4 mediate signaling by Nodal proteins during vertebrate development. *Genes Dev.* **15**, 2010-2022.
Ryan, A. K., Blumberg, B., Rodriguez-Esteban, C., Yonei-Tamura, S., Tamura, K., Tsukui, T., de la Pena, J., Sabbagh, W., Greenwald, J., Choe, S. et al. (1998). Pitx2 determines left-right asymmetry of internal organs in vertebrates. *Nature* **394**, 545-551.
Sampath, K., Cheng, A. M., Frisch, A. and Wright, C. V. (1997). Functional differences among Xenopus nodal-related genes in left-right axis determination. *Development* **124**, 3293-3302.
Sampath, K., Rubinstein, A. L., Cheng, A. M., Liang, J. O., Fekany, K., Solnica-Krezel, L., Korzh, V., Halpern, M. E. and Wright, C. V. (1998). Induction of the zebrafish ventral brain and floorplate requires cyclops/nodal signalling. *Nature* **395**, 185-189.
Shen, M. M. (2007). Nodal signaling: developmental roles and regulation. *Development* **134**, 1023-1034.
Sirotkin, H. I., Dougan, S. T., Schier, A. F. and Talbot, W. S. (2000). bozozok and squint act in parallel to specify dorsal mesoderm and anterior neuroectoderm in zebrafish. *Development* **127**, 2583-2592.
Sopory, S., Nelsen, S. M., Degnin, C., Wong, C. and Christian, J. L. (2006). Regulation of bone morphogenetic protein-4 activity by sequence elements within the prodomain. *J. Biol. Chem.* **281**, 34021-34031.
Tian, J., Yam, C., Balasundaram, G., Wang, H., Gore, A. and Sampath, K. (2003). A temperature-sensitive mutation in the nodal-related gene cyclops reveals that the floor plate is induced during gastrulation in zebrafish. *Development* **130**, 3331-3342.
Topczewska, J. M., Postovit, L. M., Margaryan, N. V., Sam, A., Hess, A. R., Wheaton, W. W., Nickoloff, B. J., Topczewski, J. and Hendrix, M. J. (2006). Embryonic and tumorigenic pathways converge via Nodal signaling: role in melanoma aggressiveness. *Nat. Med.* **12**, 925-932.
Toyama, R., O'Connell, M. L., Wright, C. V., Kuehn, M. R. and Dawid, I. B. (1995). Nodal induces ectopic goosecoid and lim1 expression and axis duplication in zebrafish. *Development* **121**, 383-391.
Williams, P. H., Hagemann, A., Gonzalez-Gaitan, M. and Smith, J. C. (2004). Visualizing long-range movement of the morphogen Xnr2 in the Xenopus embryo. *Curr. Biol.* **14**, 1916-1923.
Yan, Y. T., Liu, J. J., Luo, Y. E. C., Haltiwanger, R. S., Abate-Shen, C. and Shen, M. M. (2002). Dual roles of Cripto as a ligand and coreceptor in the nodal signaling pathway. *Mol. Cell. Biol.* **22**, 4439-4449.
Yeo, C. and Whitman, M. (2001). Nodal signals to Smads through Cripto-dependent and Cripto-independent mechanisms. *Mol. Cell* **7**, 949-957.
Yu, J. K., Holland, L. Z. and Holland, N. D. (2002). An amphioxus nodal gene (AmphiNodal) with early symmetrical expression in the organizer and mesoderm and later asymmetrical expression associated with left-right axis formation. *Evol. Dev.* **4**, 418-425.
Zhang, L., Zhou, H., Su, Y., Sun, Z., Zhang, H., Zhang, L., Zhang, Y., Ning, Y., Chen, Y. G. and Meng, A. (2004). Zebrafish Dpr2 inhibits mesoderm induction by promoting degradation of nodal receptors. *Science* **306**, 114-117.
Zhou, X., Sasaki, H., Lowe, L., Hogan, B. L. and Kuehn, M. R. (1993). Nodal is a novel TGF-beta-like gene expressed in the mouse node during gastrulation. *Nature* **361**, 543-547.